Atomic Force Microscope Vertical Feedback Control Strategy for Semi-Automated Long-Range Probe Landing

Freddy Romero Leiro, Georges Daher, Stéphane Régnier, Mokrane Boudaoud

Atomic Force Microscope Vertical Feedback Control Strategy for Semi-Automated Long-Range Probe Landing

Freddy Romero Leiro, Georges Daher, Stéphane Régnier, and Mokrane Boudaoud

***Abstract*— Traditional Atomic Force Microscopes (AFM) allow a short range displacement of the AFM probe, on the order of several tens of micrometers. When used inside an Electron Microscope (EM), the probe must be able to move on a millimeter scale with nanometer resolution. This is essential for the probe to reach any region of interest on a sample observed by an EM. In this paper, we address a challenging issue related to semi-automated long-range landing of an AFM probe on a sample. The probe is mounted on a piezoelectric inertial actuator. It is initially several millimeters away from the sample and must be safely landed to a distance on the order of hundred of nanometers (intermittent contact region). The control strategy is divided into three steps: (i) long-range velocity control using a stepping control, (ii) short and fine position control using a mixed stepping/scanning control, and (iii) position/force control using a scanning control. While traditional manual landing methods take a tremendous amount of time to complete the procedure, the proposed semi-automated method enables a safe long-range landing in less than 3 minutes. More generally, this is the first experimental demonstration in the literature of such a capability in AFM.**

I. INTRODUCTION

Atomic force microscopy (AFM) is a branch of local probe microscopy [1]. It is one of the main methods of observation and measurement at the nanoscale. When the tip of the AFM probe is sufficiently close to a surface, interaction forces between the tip and the surface appear. The dominant interactions are due to Van der Waals (VdW) forces [2]. By scanning the probe over the surface of a sample while remaining in the region of the interaction forces, the AFM is able to reconstruct the topography of the surface. In AFM, feedback control is required for probe landing and placing on the sample surface [3] [4], for scanning purposes [5][6][7][8] and to set mechanical parameters of the probe with Phase-locked loop for certain modes of operation of the AFM [9].

An AFM can be used with another microscope to help guiding the probe in a region of interest on the sample. Examples on the use of AFM tools coupled with a Light Microscope (LM) and an Electron Microscope (EM) can be found in [10] and [11] respectively. The EM providing a much better image resolution than LM, it is preferred when it comes to guide an AFM probe in a region of interest at the nanometer scale. Due to the very high magnification capability of EM, to be able to reach any region of interest on sample observed by an EM, the AFM probe must have the capability to navigate with a displacement range to resolution ratio of several million times. For instance, the AFM probe must be able to move on a distance of several mm or cm to reach any region on a sample as well as of few nm to operate in a narrow area. For this reason most of robotic systems holding probes and operating inside SEM use long-stroke actuators such as stepping piezoelectric actuators that operate in two distinct modes: low resolution stepping mode and high resolution (nanometer) scanning mode [12][13].

F. Romero Leiro, G. Daher, M. Boudaoud, and S. Régnier are with Sorbonne Université, Institut des Systèmes Intelligents et de Robotique, UMR 7222, ISIR, F-75005 Paris, France. Emails: romeroleiro@isir.upmc.fr, georges.daher@isir.upmc.fr, stephane.regnier@sorbonne-universite.fr, mokrane.boudaoud@sorbonne-universite.fr.

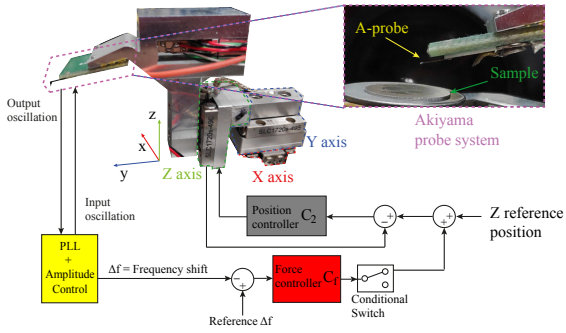

Fig. 1: Control scheme of the AFM composed of a 3-DOF serial cartesian robot and an Akiyama probe.

This paper addresses the closed-loop control of the vertical motion of an AFM probe for accurate and safe landing on a sample surface. Specifically, the work aims to implement a control strategy for long-range probe landing which is the first step when using an AFM inside an EM. Automated short-distance probe landing methods with a micrometer range displacement have been proposed in the literature. It mainly consists in controlling respectively the position and the contact force before and after the detection of the interaction forces [4]. For automated procedures, a dual stage consisting of a coarse and fine actuator connected in series can be used [3][14][15]. In [3], the phase velocity is used to detect the probe sample contact in amplitude modulation AFM. In [12], probe landing is achieved by an iterative approach alternating between fine and coarse actuation modes. A fine stage holding the AFM probe is actuated using a force and position feedback control. The coarse stage is controlled in position with an amplitude smaller than the stroke of the fine stage. The algorithm is defined in such a way that contact between the tip and the sample can only occur during the movement of the fine positioner, which guarantees a precise and safe detection of the contact. The iterative sequence of fine and coarse positioning is repeated until contact is made between the probe and the sample. The duration of this procedure depends on the initial distance

between the sample and the probe. The landing procedure can also be performed in a teleoperated manner using a haptic interface [16] or a remote control [17] [18][19]. The method proposed in this paper is divided into three steps. First, a long-range velocity control using a stepping control [20] is used for millimeter-range displacement. The speed of the probe movement is set by the user. Second, a short fine position control using a mixed stepping/scanning control [21] is implemented to provide controlled contact with nanometer range motion resolution. Finally, position and force controls complete the last step of the motion. The proposed semi-automated method allows for a safe long distance landing of the AFM probe in less than 3 minutes.

The paper is structured as follows. Section II describes the experimental setup. The vertical tip landing strategy is presented in section III and the control methodologies in sections IV, V and VI. Experimental results are shown and discussed in section VII. Section VIII concludes the paper.

II. Experimental setup

The system includes a 3-DOF serial cartesian robot (Fig.1). All its axes use the same type of piezo-electric stick-slip (PSS) actuators which can be controlled in two modes: stepping mode, where a sawtooth signal produces a stick-slip motion; and scanning mode, where the actuator is moved using a smooth voltage in order to avoid the stick-slip action. The stick-slip mode allows the axis to move with a stroke of 12 mm, while the scanning mode is used for precise positioning at nanometer resolution and a maximum range of 1.6 µm. All axes have an integrated laser encoder position sensor with 5 nm of resolution. This device has been modeled in [12]. Several control strategies dedicated for PSS type actuators that are partially used in this paper have been proposed in previous works [20][22][23].

The robot is used as a nano-positioning device to perform atomic force microscopy (AFM). It is equipped with an Akiyama probe (A-probe), as shown in Fig.1. The A-probe is designed to perform Frequency Modulated AFM (FM-AFM) and it is best suited for operation in the intermittent contact region [9]. The A-probe is composed of two elements: a quartz tuning fork through which the probe is actuated with a voltage signal and a cantilever with a sharp tip attached to both arms of the tuning fork. The A-probe works by the principle of self-sensing using the piezo-electric quartz tuning fork [9]. The driving signal of the A-probe is controlled using a Amplitude control loop and a Phase Lock Loop (PLL) working in parallel to keep the driving frequency at the resonant frequency of the probe at all times during its interaction with the surface. The output of the PLL is the frequency shift Δf of the A-probe's resonance with respect to its free resonant frequency. Once the A-probe is located in the intermittent contact region, the AFM is performed by keeping constant Δf with a force control loop on the Z-axis of the cartesian robot. Also, as shown in Fig.1, position and force controllers are designed to perform AFM imaging. The force control loop is only engaged when the A-probe is located in the intermittent contact region. Outside this region, the Z-axis is controlled only in position. The position at which the A-probe stabilizes in the intermittent contact region depends on the reference Δf chosen in the force control loop and the amplitude of oscillation of the probe. In addition to the information provided by Δf, the user has a live video feed of the position of the A-probe through a side-mounted camera (Fig.2)

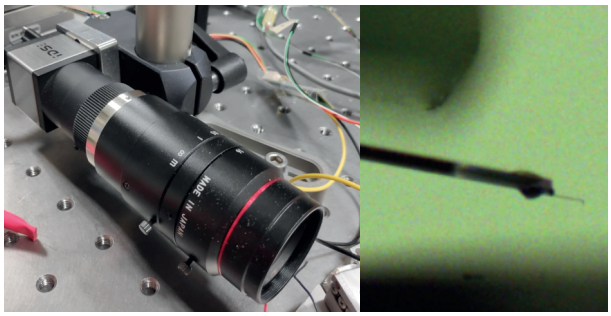

Fig. 2: Camera used for the live video and side view of the probe.

III. Vertical long-range control strategy

The method consists of four steps. Each controller is detailed later in the article:

Step I **(Velocity stepping mode control)**: The Z axis is controlled in stepping mode using a sawtooth voltage whose frequency is adjusted by a proportional controller. This strategy is a variation of the of the f/u proportional controller first proposed in [24]. In this Step, the user can control the probe approach speed. The switch to Step II is made by the user when she/he considers that the probe is close enough to the surface relying on the camera feedback.

Step II **(Position mixed stepping/scanning mode control)**: The stroke of the actuator in scanning mode being limited to 1.6 μm, it is necessary to alternatively apply a stepping mode controller to allow a long distance positioning while having the possibility to realise a very precise positioning in scanning mode. In Step II, the strategy consists then in a mixed mode of stepping and scanning control. The mixed controller is designed so that contact between the probe and the sample can only occur during scanning control. When contact is made, the controller of Step II switches to Step III. The switching condition is defined by the frequency shift of the A-probe. The switch from Step II to Step III is performed using a smooth transfer strategy, i.e. bumpless.

Step III **(Position/force scanning mode control)**: the tip is positioned in the intermittent contact region. The user can chose to stay in Z-position control or to activate the force control loop. Once engaged, the force controller keeps the frequency shift of the A-probe constant and makes the system ready to perform an AFM scan.

Step I is a good option to speed up the globale long-range vertical motion process but it must switch to step II well before the contact for safety reasons. In Step II, the speed of the operation can not be as fast as in Step I, but the strategy allows a safer contact detection. In the following, each controller involved in steps I, II and III is described.

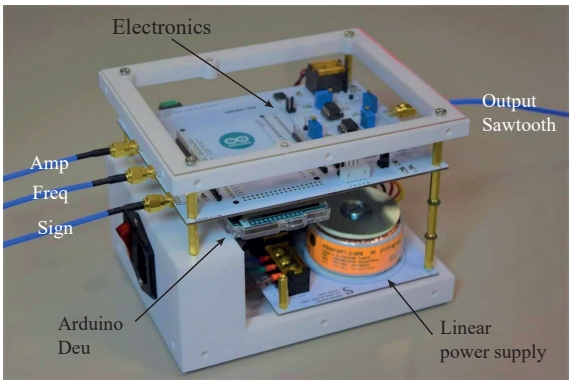

Fig. 3: Home made sawtooth generator used for stepping mode control. The analog inputs named Amp, Freq, and Sign, control the amplitude, frequency and direction respectively of the sawtooth output voltage.

IV. Control for Long-Distance Approach

To control the position and velocity of the Z-axis in stepping mode, a home-made sawtooth generator is designed. It is based on an Arduino Due development board (Fig.3). The parameters of direction (sign), frequency and amplitude of the sawtooth signal are controlled using three independent analog signals. The sawtooth amplitude can range from 0 to 5 V. This voltage is then amplified 20 $\times$ before powering the actuator. The frequency signal can range from 20 Hz to 20 kHz by controlling an analog input signal ranging from 0 to 3.8 V. A proportional frequency controller is designed using Matlab/Simulink and implemented using a dSPACE control board. The structure of the controller is shown in Fig.4. The gain K_f is set to 1 and the amplitude of the sawtooth voltage is kept at 5 V before amplification. Fig.5 shows experimental results of the closed loop displacement of the actuator using the controller when tracking of a 1 Hz and 2 μm sinusoidal reference signal. The positioning error is less than 20 nm.

A control of the amplitude of the sawtooth signal is not needed because when the Z-position is close to the set-point, the error signal changes sign back and forward rapidly. This changes the direction of the sawtooth signal while the frequency is reduced, making the signal flatter with a reduced amplitude. The net result is a control signal that is no longer a pure sawtooth, and whose frequency and amplitude change in response to the position error. This indirect amplitude control mechanism is illustrated in Fig.6. Since the initial distance between the probe and the surface is not known precisely, it is not intuitive to define a position reference for the closed

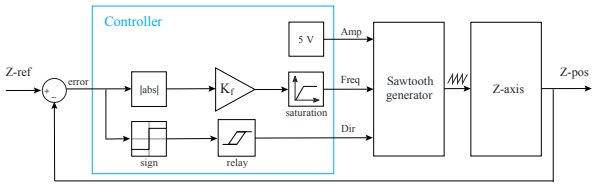

Fig. 4: Block diagram of the frequency proportional controller for long-range approach.

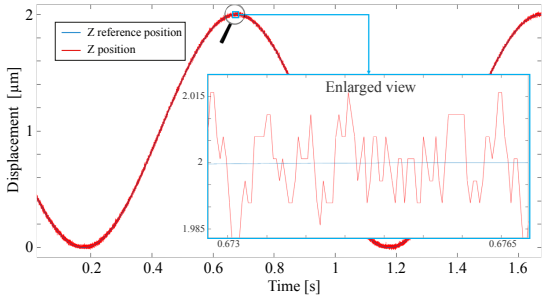

Fig. 5: Experimental results of the proportional frequency controller. Closed loop position of the Z axis while tracking a 1 Hz and 2 µm sinusoidal reference position signal.

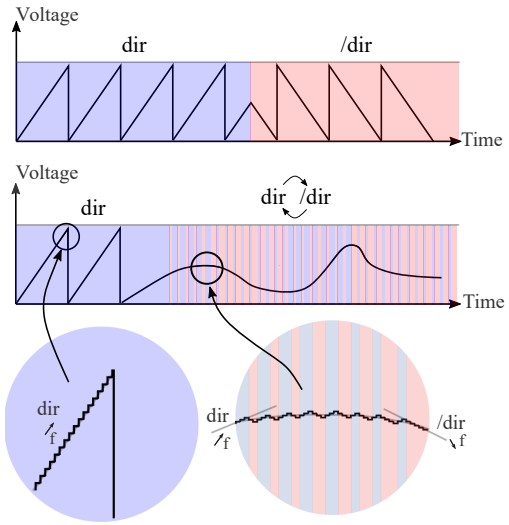

Fig. 6: Indirect control of the amplitude of the sawtooth voltage by sign switching and frequency control.

loop system. Therefore, providing a velocity reference while imposing a linear motion for the actuator is more intuitive to a user. It is a much better way to control the approach. This is done by introducing an integrator into the setpoint (Fig.7). Therefore, the user controls the speed and direction of motion of the probe (ascent or descent) by controlling the magnitude and sign of the integrator input, respectively. The integrator state is reset to 0 each time the controller is disconnected to avoid wind-up and saturation. Also, when the controller is connected, the position at that moment is kept as the new initial position by using a *signal hold* block. This is to prevent the Z-axis from jumping to the last previous reference when reconnecting. In section VII, this control structure will be referred as the *Stepping controller*. A direct velocity feedback is not used because the velocity signal provided by the sensor in stepping motion is very noisy [20].

V. Control for Short-Distance Approach

The stepping mode involves stick and slip movements of the actuator. Each slip causes strong oscillations on the AFM probe. During the Z descent, these rapid position changes caused by the sawtooth signal can damage or destroy the probe. Therefore, we must ensure that the contact between

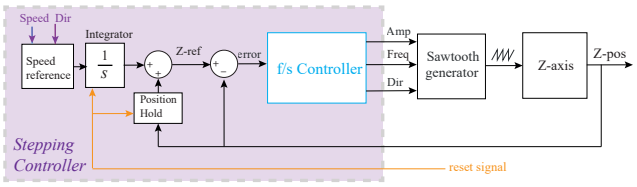

Fig. 7: Velocity stepping control scheme.

the probe and the surface is made in scanning mode which is much more accurate and controllable. However, in scanning mode, the actuator has a limited range of 1.6 µm. Hence, a mixed stepping/scanning mode control is devised (Fig.8).

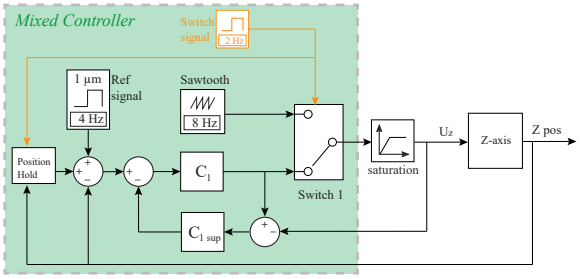

Fig. 8: Block diagram of the mixed stepping/scanning control scheme.

Based on the experimental step response of the actuator, the transfer between the input voltage and the actuator position is identified as follows:

$$G_z = \frac{0.0135}{8.687\times10^{-10}s^2 + 1.768\times10^{-5}s + 1}\ \mu m/V \qquad (1)$$

The position controller C_1 is designed based on G_z and pole-zero cancellation with integral action. It allows an open loop gain crossover frequency (unity-gain frequency) of 4 Hz. It is intentionally designed to be slow for a safe probe sample contact detection. The transfer function of C_1 is:

$$C_1 = \frac{1}{G_z}\left(\frac{2013}{s(s+159.7)}\right) \qquad (2)$$

The actuation signal U_z (Fig.8) alternates between a 8 Hz sawtooth signal and the output of C_1. The switch between the two signals is done smoothly through the supervisor C_{1sup} which makes sure that the output of C_1 is equal to that of the sawtooth when disconnected. When C_1 is active, the input reference position is a 4 Hz square signal of 1 µm of amplitude. The switching condition is controlled by a 2 Hz square signal. It also controls a *signal hold* block which sums to the position setpoint. This is added so that the reference position signal is given with respect to the new Z-position after the stepping positions caused by the sawtooth signal. The amplitude of the sawtooth signal is set to 22 V after amplification. The experimental controlled position of the Z axis with the mixed stepping/scanning actuation mode is shown in Fig.9. The maximum amplitude of Z during the scanning control is always higher then the maximum amplitude of the next stepping motion. This difference in amplitude is the safety margin as shown in Fig.9. In this way,

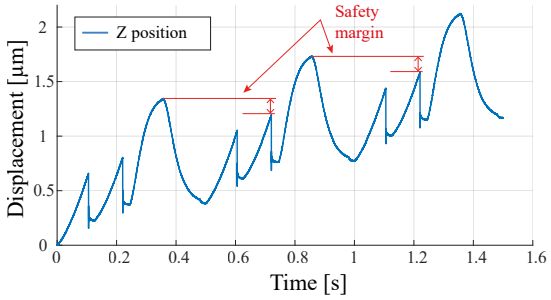

Fig. 9: Experimental measurements of the controlled Z-axis position during the mixed stepping/scanning motion.

we ensure that the contact between the probe and the surface will occur during the scanning mode control and never in stepping mode. In section VII, this control structure will be referred as the *Mixed controller*.

VI. Bumpless Contact and Force Control

To allow a smooth A-probe/sample contact, the control laws must pass smoothly from Step II (Fig.8) to Step III (Fig.1). The control structure that is in charge for a bumpless switching is shown in Fig.10. The switching conditions are defined on the basis of the user's decision to engage the mixed stepping/scanning sequence (Step II), and the frequency shift Δf signal coming from the PLL. In the latter case, when Δf reaches 40 Hz, a transition between Step II and III happens by switching the output from C_1 to C_2. The detailed control scheme of Step III is also shown in Fig.10.

The position controller C_2 is designed based on pole-zero cancellation with integral action. It allows an open loop gain crossover frequency of 1 kHz. It is much faster than C_1. This high bandwidth is necessary because C_2 is used for fast AFM imaging. The transfer function of C_2 is:

$$C_2 = \frac{1}{G_z}\left(\frac{5.032\times10^8}{s(s+7.984\times10^4)}\right) \qquad (3)$$

The switch between C_1 to C_2 is done smoothly thanks to the supervisor $C_{2\,sup}$.

In section VII, this control structure will be referred as the *Scanning controller*. Finally, in order to perform an AFM for topography, the vertical long-range probe landing must end with a force control. The aim is to keep the frequency shift Δf at a constant value. For this purpose, a force

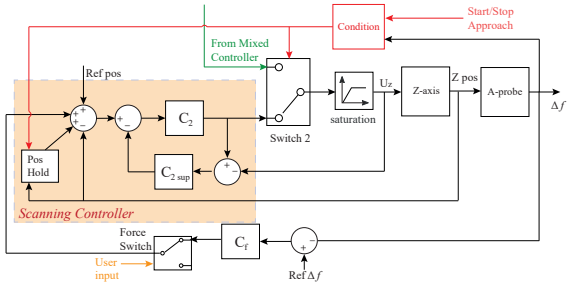

Fig. 10: Block diagram of the scanning controller and force controller with bumpless switching.

controller C_f is designed based on the transfer function between the position of the Z axis and Δf. This model, identified experimentally, is defined as follows:

$$G_{ak} = \frac{378.7}{1.759\times10^{-8}s^2 + 9.284\times10^{-5}s + 1} \text{ Hz/µm} \quad (4)$$

C_f is designed based on pole-zero cancellation, considering G_{ak}, with integral action. It allows an open loop gain crossover frequency of 150 Hz. Its transfer function is:

$$C_f = \frac{0.036s^2 + 1.289s + 5131}{s(s+1812)} \quad (5)$$

C_f is activated by the user once the tip is in the intermittent contact region after performing bumpless contact.

VII. Control Implementation and Experimental Results

A. Implementation of the control scheme

The block diagram showing all the controllers, the home-made sawtooth generator, the Z-axis and the A-probe is shown in Fig.11. The control scheme is implemented using dSpace DS1007 board running at 25 kHz. The Steps II and III are designed using digital control schemes, represented by the *Mixed controller* and *Scanning controller* blocks respectively in Fig.11. This is different from Step I control structure where the output of the *Stepping controller* is from the sawtooth generator. The latter generates a signal whose frequency can reach 20 kHz, exceeding the Shannon frequency of the card. For this reason, the transition from the stepping controller to the other two is not as smooth as the transition between the mixed controller and the scanning controller. The switch from the analog sawtooth generator output to the dSpace voltage output U_z is done by an analog multiplexer (MUX in Fig.11). While the stepping controller is running, the controllers C_1 (Fig.8) and C_2 (Fig.10) have their outputs set to 0 through the supervisors $C_{1\,sup}$ and $C_{2\,sup}$. The switch from the stepping controller is done while the approach speed is close to 0. Hence, the output of C_1 and C_2 are close to the output of the sawtooth generator at that instant, so the jump is small. This is not critical because at this point, the A-probe tip is far from contact. Also, when switching from Step I, the approaching sequence will not start immediately, the controller connected by default is the scanning controller with a set position at zero. The

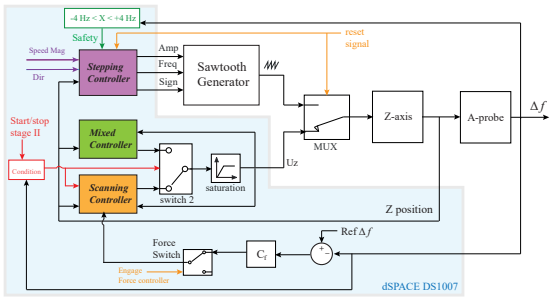

Fig. 11: Block diagram of the complete long-range probe-landing control scheme.

system will remain in this state until the user decides to start the mixed stepping/scanning approach sequence. Finally, to avoid any contact between the probe and the surface during the long-range motion, the approach speed is set to zero whenever Δf is outside a window of ±4 Hz.

B. Experimental Results

The complete experimental displacement of the Z-axis during the long-range probe landing is shown in Fig.12 (a). The three Steps of approach as well as the transitions between Steps are visible. Here, we see that the user changes the speed of the long-range approach, starting with a fast approach of 100 µm/s, then reducing it to 50 µm/s, and finalizing at 5 µm/s before stopping once the signal Δf is close to -3 Hz. At this point, the user switches to the next step by closing the MUX. In Fig.12 (b), the jump in Z-position generated by the switch from the stepping controller to the scanning controller is around 200 nm. This small jump is acceptable given that at this point the tip of the A-probe is still about tens of µm from contact. What follows is a short waiting time until the user decides to engage the mixed controller. The Z-axis proceeds to perform the mixed stepping/scanning movement until the signal from the A-probe reaches the desired threshold (40 Hz) in the intermittent contact region. As shown in Fig.12 (c), once the threshold is reached, the switching from the mixed controller to the scanning controller happens smoothly without any noticeable jump in the Z-axis position. This is corroborated in Fig12 (e) where Δf reaches 40 Hz and stays around this value after the bumpless transfer. Now that the A-probe's tip is in the intermittent contact region, the force controller C_f is engaged manually by the user (Fig.12 (d)). As seen in Fig.12 (f), Δf proceeds to stabilize around 70 Hz. Initially, the probe was at a distance of $\approx$ 2.5 mm from the surface. In less than 3 minutes, the system is ready for AFM imaging.

VIII. Conclusions

In this study, a vertical feedback control strategy is proposed for semi-automatic probe landing of a long range AFM. The method has been described and guidelines have been proposed. The control strategy has been successfully tested experimentally. The A-probe started its travel from a distance of 2.5 mm and has been landed smoothly avoiding damage in less than 3 min. It has been possible to stabilise the frequency shift of the A-probe at 70 Hz, which is equivalent to a 130 nm positioning within the intermittent contact region. The procedure consisted of three steps. Step I is a long-range approach in which the user can control the approach speed at will while seeing at the video feed of a side-view camera. Once the probe-surface distance is judged to be within tens of micrometers, the user switches to Step II. The short-range approach has been done automatically using a mixed stepping/scanning motion. At the end, the tip-surface contact is reached smoothly using a bumpless transfer control strategy. In Step III, a force control is activated which maintains Δf constant. At this point, the system is ready to perform AFM imaging. This is the first time that this

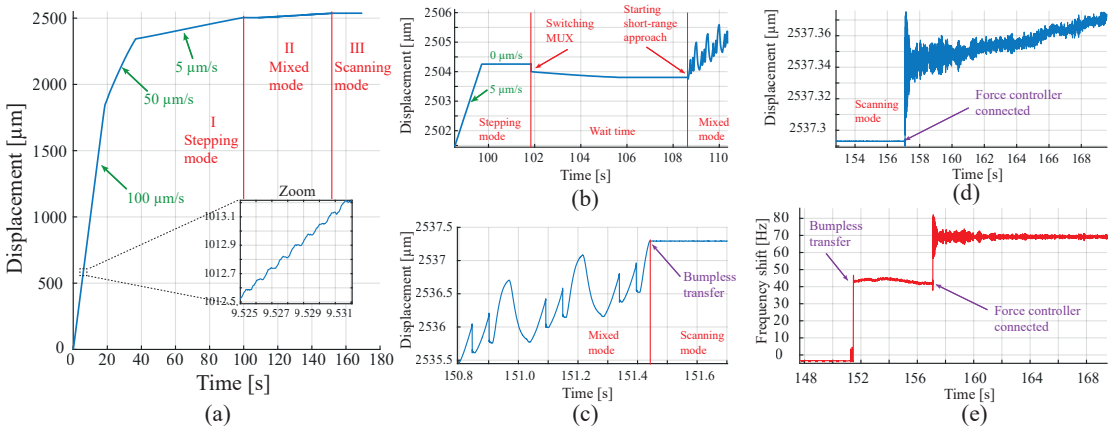

Fig. 12: Experimental results of the long-range tip landing procedure: a) Complete travel of the Z-axis during tip landing. b) Transition from stepping mode to mixed stepping/scanning mode. c) Bumpless transition from mixed stepping/scanning mode to scanning mode. d) Activation of the force control loop. e) Effect of the bumpless transition and force control loop activation on A-probe's frequency shift.

capability is demonstrated. Here, the AFM is not inside an electron microscope (EM), but the robot used in this study and the A-probe are designed to operate in EM. The results obtained in this paper will significantly accelerate the AFM process in the EM domain, where long-range positioning and landing is an essential prerequisite.

IX. ACKNOWLEDGMENTS

This work has been sponsored by the ANR project Robine (ANR-19-CE33-0005).-

REFERENCES

[1] G. Binnig, C. F. Quate, and Ch. Gerber. Atomic force microscope. *Phys. Rev. Lett.*, 56:930–933, 1986.

[2] B Bhushan. *Springer handbook of nanotechnology*. Springer, 2017.

[3] S. Belikov, J. Alexander, M. Surtchev, I. Malovichko, and S. Magonov. Automatic probe landing in atomic force microscopy resonance modes. In *American Control Conference (ACC)*, 2017.

[4] Jonathan Cailliez, Mokrane Boudaoud, Shuai Liang, and Stéphane Régnier. Robust hybrid control of an atomic force microscope for the characterization of interaction force regions at the nanoscale. *IEEE Transactions on Control Systems Technology*, 29(4):1689–1703, 2021.

[5] A. J. Fleming, S. S. Aphale, and S. O. R. Moheimani. A new method for robust damping and tracking control of scanning probe microscope positioning stages. *IEEE Transactions on Nanotechnology*, 9:438–448, 2010.

[6] M. R. P. Ragazzon, M. G. Ruppert, D. M. Harcombe, A. J. Fleming, and J. T. Gravdahl. Lyapunov estimator for high-speed demodulation in dynamic mode atomic force microscopy. *IEEE Transactions on Control Systems Technology*, 26(2):765–772, 2018.

[7] Ali Mohammadi, Anthony G. Fowler, Yuen K. Yong, and S. O. Reza Moheimani. A feedback controlled mems nanopositioner for on-chip high-speed afm. *Journal of Microelectromechanical Systems*, 23(3):610–619, 2014.

[8] A Bazaei, Y K Yong, and S. O. R Moheimani. Combining spiral scanning and internal model control for sequential afm imaging at video rate. *IEEE/ASME Transactions on Mechatronics*, 22(1):371–380, 2017.

[9] T Akiyama, N F. de Rooij, U Staufer, M Detterbeck, D Braendlin, S Waldmeier, and M Scheidiger. Implementation and characterization of a quartz tuning fork based probe consisted of discrete resonators for dynamic mode atomic force microscopy. *Review of Scientific Instruments*, 81(6):063706, 2010.

[10] Chaoyang Shi, Devin K Luu, Qinmin Yang, Jun Liu, Jun Chen, Changhai Ru, Shaorong Xie, Jun Luo, Ji Ge, and Yu Sun. Recent advances in nanorobotic manipulation inside scanning electron microscopes. *Microsystems and Nanoengineering*, (16024), 2016.

[11] Eiji Usukura, Akihiro Narita, Akira Yagi, Shuichi Ito, and Jiro Usukura. An unroofing method to observe the cytoskeleton directly at molecular resolution using atomic force microscopy. *Nature Scientific Report*, doi 10.1038/srep27472, 2016.

[12] Mokrane Boudaoud, Tianming Lu, Shuai Liang, Raouia Oubellil, and Stéphane Régnier. A voltage/frequency modeling for a multi-dofs serial nanorobotic system based on piezoelectric inertial actuators. *IEEE/ASME Transactions on Mechatronics*, 23(6):2814–2824, 2018.

[13] Tianming Lu, Mokrane Boudaoud, David Hériban, and Stephane Régnier. Nonlinear modeling for a class of nano-robotic systems using piezoelectric stick-slip actuators. In *International Conference on Intelligent Robots and Systems (IROS)*, 2015.

[14] Andrew J. Fleming. Dual-stage vertical feedback for high-speed scanning probe microscopy. *IEEE Transactions on Control Systems Technology*, 19(1):156–165, 2011.

[15] Sergey B, John A, Marko S, and Sergei M. Digital q-control and automatic probe landing in amplitude modulation phase imaging afm mode. *IFAC-PapersOnLine*, 2017.

[16] A. Bolopion, H. Xie, D. S. Haliyo, and S. Regnier. Haptic teleoperation for 3-d microassembly of spherical objects. *IEEE/ASME Transactions on Mechatronics*, 17(1):116–127, 2012.

[17] J-O.Abrahamians, B.Sauvet, J.Polesel-Maris, R.Braive, and S.Régnier. A nanorobotic system for in situ stiffness measurements on membranes. *IEEE Transactions on Robotics*, 30:119–124, 2013.

[18] Z. Gong, B. K. Chen, J. Liu, and Y. Sun. Robotic probing of nanostructures inside scanning electron microscopy. *IEEE Transactions on Robotics*, 30(3):758–765, 2014.

[19] C. Ru, Y. Zhang, Y. Sun, Y. Zhong, X. Sun, D. Hoyle, and I. Cotton. Automated four-point probe measurement of nanowires inside a scanning electron microscope. *IEEE Transactions on Nanotechnology*, 10(4):674–681, 2011.

[20] Shuai Liang, Mokrane Boudaoud, Barthélémy Cagneau, and Stéphane Régnier. Velocity characterization and control strategies for nanorobotic systems based on piezoelectric stick-slip actuators. In *IEEE International Conference on Robotics and Automation (ICRA)*, 2017.

[21] R. Oubellil, A. Voda, M. Boudaoud, and S. Régnier. Mixed stepping/scanning mode control of stick-slip sem-integrated nano-robotic systems. *Sensors and Actuators A: Physical*, 285:258–268, 2019.

[22] Raouia Oubellil, Alina Voda, Mokrane Boudaoud, and Stéphane Régnier. A 2-dof h∞ control strategy for a 3 axes robotic system operating at the nanometer scale. In *International Conference on System Theory, Control and Computing (ICSTCC)*, 2016.

[23] Raouia Oubellil, Alina Voda, Mokrane Boudaoud, and Stéphane Régnier. Robust control strategies of stick-slip type actuators for fast and accurate nanopositioning operations in scanning mode. In *Mediterranean Conference on Control and Automation (MED)*, 2015.

[24] Micky Rakotondrabe, Yassine Haddab, and Philippe Lutz. Voltage/frequency proportional control of stick-slip micropositioning systems. *IEEE Transactions on Control Systems Technology*, 16(6):1316–1322, November 2008.